Structure/ Reactivity study of model and biodiesel soot in DPF regeneration conditions

Ophélie Pereira

Chemical Engineering Department, Instituto Superior Técnico, Av. Rovisco Pais, 1, 1049-001 Lisboa, Portugal
Sorbonne Université, Institut Jean Le Rond D´Alembert, 2 place de la gare de Ceinture, 78210 Saint Cyr l´Ecole, France

ARTICLE INFO	ABSTRACT
	This study aimed to evaluate the effect of oxygenated compounds concentration and the length of their carbon chains, on the structure and reactivity of soot. These particles, which were obtained from diesel/biodiesel surrogates, in an atmospheric Santoro-type burner with a diffusion flame, were called "model" particles. A comparative analysis was carried out between "model" samples and soot produced on an engine bench, representative of heavy-duty vehicle engine. Soot characteristics were studied through diverse techniques, such as laser granulometry, elemental analysis (CHNS/O), thermogravimetric analysis (TGA), Raman spectroscopy and transmission electron microscopy (TEM). Higher content and/or carbon chain length of the studied compounds promoted the formation of smaller particles. Oxygen and soluble organic fraction (SOF) content in soot samples decreased with higher concentration and/or chain length. No significant dissimilarities were registered in the graphitic structures. Temperature programmed oxidations (TPO) were performed to correlate soot composition and structure with oxidation reactivity. Soot originated by higher concentrations of additives revealed a lower reactivity. During a catalytic study, the impact of the presence of MnO_x-CeO_2- type catalyst on soot oxidation was analysed. The temperature to obtain 10% of carbon conversion showed considerable modifications. The decrease of temperature in the case of "real" soot was probably due to the oxidation of the soluble organic fraction. The synergetic effect of oxygen and nitrogen dioxide was evaluated. Finally, the impact of the soot-catalyst contact was assessed. Generally, the obtained results revealed that "model" particles had a structure and reactivity comparable to particles produced in real conditions.

1. Introduction

Liquid fuels are the most widely used energy resource by world´s population. Unfortunately, their development has been accompanied by numerous issues from the environmental point of view, representing the major emission source of greenhouse gases (GHG) in the automobile sector [1,2]. Consequently, new procedures and increasingly stringent *Euro standards* [3] have been implemented to control the current situation. Additionally, the scientific community has worked to find alternative sustainable and more efficient sources of energy, which generate reduced emissions. Biofuels have emerged as one of the most strategically important fuel sources. Their use becomes a solution to limit GHG emissions, improve air quality and prevent global warming. In fact, CO_2 emission can be reduced by 78%, CO by 46,7%, HCs by 45,2% and PM by 66,7% when compared with fossil fuel [4].

Biodiesel, composed by long carbonaceous chains highly saturated in alkyl esters, is produced from vegetable oils or animal fats, through transesterification reactions. In compression-ignition engines, it is mostly used in diesel blends. However, it can completely replace diesel fuel in some heavy-duty vehicles that run exclusively with pure biodiesel. Due to the complex composition of biodiesel fuels, surrogate mixtures are generally used in comparative studies between diesel and biodiesel. They have a well-known chemical composition leading to a better identification of the different factors that govern biodiesel combustion process in diesel engines and affect pollutant emissions. Due to the uncertainty about biodiesel effect on pollutant emissions, numerous studies have been carried out [5-7]. Among them, several works are focused on the impact of particulate matter, especially soot, considered as one of the major emissions in diesel engines.

Nowadays, Diesel Particulate Filters (DPF) are adopted to manage particulate emissions. Among the different available configurations, *wall-flow* type filters are the most common. They are honeycomb monoliths with parallel channels plugged alternatively at each end to force the exhaust gas to flow through the porous filter wall, where soot is retained [8,9]. As the accumulated soot in the filter increases, the back pressure also increases, and it will progressively originate a decrease of engine power, penalizing the fuel consumption. To restore the filter efficiency, it must be cleaned through a regeneration process [10,11]. Sometimes the exhaust gas temperature can drop to a point where continuous regeneration can no longer be completely guaranteed. In this case, active regeneration is required with introduction of an additional thermal energy. Through a thermic and periodic regeneration, the heat release is enough to raise the exhaust temperature of the particulate filter. As a result, the deposited diesel soot oxidizes with the surplus oxygen present in the exhaust gas.

However, the DPF regeneration performance depends on soot oxidation reactivity. In turn, this can be affected by characteristics such as composition, structure and morphology of soot particles. These properties, which are specific for each soot, depend on their origin and production conditions.

Several investigations have been conducted to determine the major factor responsible for the reactivity observed in diesel/ biodiesel soot particles. In previous studies, a notorious reduction of soot emissions was observed when using biodiesel or biodiesel blends. This phenomenon was explained by the predominance of soot oxidation over its formation, due to the abundance of oxygenated radicals produced during the pyrolysis process [12-14]. Results of Flynn *et al.* [15] investigations showed some decrease in the formation of soot precursors when increasing the oxygen content in the fuel. They justified this tendency explaining that large fractions of fuel carbon were directly converted to CO/CO_2, leading to fewer carbons available for precursors formation. Schmidt and Van Gerpen [16] justified soot emissions decrease by the low aromatic content when blending petroleum diesel with methyl ester-based biofuel. Mueller *et al.* [17] concluded that oxidation rate of biodiesel soot was up to six times higher than the diesel soot one. They detected on biodiesel soot samples the presence of carbon-oxygen functional groups like C=O, C-O-C or C-OH, which promote soot oxidation.

Moreover, diverse research [18-21] evidenced the influence of particles chemical structure on their reactivity via number and location of carbon active sites. Indeed, reactivity has been found to be higher on carbon surfaces containing many exposed edge sites. The loss of reactivity in particles with higher degree of graphitisation was explained by the fact that graphitised carbons have longer graphene layers and, therefore, a lower proportion of atoms in edge positions. In other studies, it was found that the presence of oxygen functional groups on the particles surface could enhance soot reactivity [22].

It is difficult to ensure that the soot collected in the DPF is completely burned at low exhaust temperature. On the other hand, soot combustion at high temperature (>500ºC) can lead to a larger energy consumption [23,24]. Thus, the advanced catalysts coated on DPF have been widely investigated to decrease the temperature of soot combustion [25-27].

Many catalysts have been reported for soot oxidation. Among the tested single oxides in combustion, CeO_2 is one of the most studied. Ceria oxide exhibits excellent catalytic activities due to its special oxygen storage capacity [28,29]. On the other hand, manganese oxide also has been used in oxidation reactions due to its strong oxidative property. The high activity of Mn is attributed to the element´s multivalent oxidation states (mainly Mn^{2+}, Mn^{3+} and Mn^{4+}) and to the high mobility of lattice oxygen. Therefore, catalysts containing such elements as manganese and cerium belong to the most promising ones [30-32]. Compared with pure CeO_2 and MnO_x, MnO_x-CeO_2 catalyst has showed higher efficiency owing to the strong synergetic effect between the bimetal oxides in the solid solution. Soot oxidation temperatures are much lower, and the oxidation rates are significantly higher in presence of these mixed oxides. It has been proved that they exhibit a high activity for NO-assisted soot oxidation. This can be explained by the ability to store NO at low temperature in form of nitrates, followed by a release of NO_2 as a strong oxidizing agent, through the decomposition of those nitrates [33]. Furthermore, it has been found that the decomposition of nitrates results in not only the production of NO_2 but also in the desorption of active oxygen, which plays a key role on the promotion of soot oxidation. [34]

The aim of this work is to widen the current knowledge about the reactivity of soot. It is focused on the comparison between particles produced with an academic burner of Santoro [35], which are classified as "models", and particles resulting from the combustion of fuel on an engine bench**,** which is representative of an engine on a heavy-duty vehicle on road (Renault-Volvo Trucks). These last ones are classified as "real" soot. Given the fact that trucks operate with diesel fuel, use of biodiesel as an alternative to diesel is investigated. Along this study, the influence of different structures of ester molecules present in biodiesel and different concentration of these compounds, on soot composition and structure is investigated. Then, soot properties are correlated with soot oxidative reactivity. Furthermore, with the aim to improve the efficiency of Diesel Particulate Filters and consequently to reduce soot emissions, the regeneration process is studied as well as the interaction between a catalyst and soot.
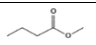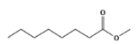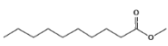
2. Experimental

2.1. Test soot

In the present study, due to the complexity of diesel composition, a diesel surrogate «Aref», consisting of a binary mixture of 70% (in mole%) of n-decane and 30% of α-methylnaphthalene (α-MN), was used to produce "model" diesel soot. This surrogate was already used in many studies to simulate combustion in diesel engines and was tested to reproduce the soot formation process during the combustion of commercial diesel [36,37]. "Model" biodiesel was prepared by adding oxygenated additives to the reference surrogate «Aref», namely methyl butanoate, methyl octanoate and methyl decanoate, in two different proportions (7 and 30 mole%). Obtained surrogates were named «MB7», «MB30», «MO7», «MO30», «MD7» and «MD30», respectively. Simple compounds of high purity were used to produce biodiesel surrogates, which are representative of real biodiesel, to better understand the different factors affecting biodiesel combustion in diesel engines and consequently, their soot emission and reactivity.

Table 1 shows the produced surrogates with their correspondent chemical composition, while Table 2 exhibits the chemical formula and structure of the studied methyl ester-based additives.

Table 1. Composition of Diesel and Biodiesel surrogates.

Surrogate	Composition (mole%)	Additive (mole%)
Aref	70% n-decane + 30% α-methylnaphthalene	-
MB MO MD	Aref + methyl butanoate Aref + methyl octanoate Aref + methyl decanoate	7% and 30%

Table 2. Chemical formula and structure of methyl ester-based additives used for Biodiesel surrogates.

Methyl ester	Chemical formula	Structure
Methyl butanoate	$C_5H_{10}O_2$	
Methyl octanoate	$C_9H_{18}O_2$	
Methyl decanoate	$C_{11}H_{22}O_2$	

"Model" soot was produced through an incomplete combustion in a previous work [38] in non-premixed diffusion

flames over an axisymmetric co-flow burner (*Santoro* burner [39,40]) at atmospheric pressure.

"Real" soot was provided by Renault-Volvo Trucks. The DPF was placed downstream of a Diesel Oxidation Catalyst (DOC) to ensure the removal of adsorbed hydrocarbons. The system worked with a low loading cycle operating at low temperatures, which is representative of very severe cold real drive cycles. Temperature of exhaust gases upstream the filter was 160ºC. Particles of soot (B7-BM and B100-BM) were produced by combustion of fuel with 7% and 100% (volume), respectively, of methyl ester from rapeseed oil. The used diesel fuel was a standard *Euro VI* fuel (EN 590).

2.2. Soot particles characterization

2.2.1. Laser particle size analysis

Measurement of particle size distribution of soot aggregates was carried out fully automatically by an *ANALYSETTE22 FRITSCH NanoTec,* under wet dispersion in which water was used as a suitable liquid. In this equipment, the sample is continuously recirculated and dispersed in a close circulatory system unit. For the support of the dispersion process, an integrated ultrasonic generator is used, and the intensity is adjustable via operating software (*MaS control*). The total measuring range of 0,01-2100 µm can be detected by the combination of two laser beams. An infrared laser (λ= 532 nm) is responsible for measuring large particles, while the measurement of the smallest particles down into the nano-range is performed by a green laser (λ= 850 nm). The measurement is automatically launched since the quantity of soot is enough to have a value of adsorbed beam between 7% and 15%. Before each experiment, a surfactant (*Dusazin 901*) and water were added to the soot sample, to ensure a complete dispersion of the particles.

2.2.2. Elemental analysis: CHNS/O

This analysis was performed with a *Thermo Fisher Scientific Flash 2000* analyser. The elemental composition of soot samples was determined in terms of organic compounds: carbon (C), hydrogen (H), nitrogen (N), sulfur (S) and oxygen (O). For the CHNS analysis, samples were weighed in a tin capsule and introduced into the combustion reactor (950-1000ºC) via a *Thermo Scientific MAS 200R Autosampler*. The resulted gases (CO_2, H_2O, N_2 and SO_2, respectively) were separated by a chromatographic column (GC) and detected by a thermal conductivity detector (TCD). For oxygen determination, the sample was weighed in a silver capsule and the system operated in pyrolysis mode. The reactor contained nickel coated carbon maintained at 1060°C. The oxygen present in the sample, combined with the carbon, formed carbon monoxide which was then separated from other products and detected.

2.2.3. Thermogravimetric analysis (TGA)

Two types of thermogravimetric analysis were performed with about 5 mg of soot, placed in a thermo-balance (*TA TGA Q500*) and heated until a targeted temperature with a 5ºC/min ramp, under a gaseous mixture with a predefined concentration. TGA under air up to 700ºC was executed to measure the ash content in the soot samples. TGA under nitrogen up to 400ºC, with a 4 h stage, was used to measure volatile and adsorbed organic compounds. The mass loss observed at temperatures lower than 110ºC was assumed to be due to the desorption of water and poorly chemisorbed compounds.

2.2.4. Raman spectroscopy

Raman spectroscopy measurements were performed with a Raman Microsystem (*Horbina Jobin Yvon HR 800 UV*), operating with a green sourced laser excitation at 532 nm. The output power was fixed at 0,1 mW in the scanning range of 800-3500 cm^{-1}. The spectrometer included a grating with 600 grooves.mm^{-1} and a CCD detector with 50× magnification objective lens.

2.2.5. Transmission electron microscopy (TEM)

A tungsten-filament 100kV transmission electron microscope (*JEOL JEM 100CX)*, with a point resolution of 3Å, was used for analysis of the internal structure of soot particles. The high-resolution images were acquired under 500,000× magnification and were treated on *Image J®*, allowing the measurement of graphene layer planes length as well as the interlayer distance.

2.3. Temperature programmed oxidation (TPO)

2.3.1. Non-catalytic oxidation

Soot reactivity was studied by performing temperature programmed oxidation experiments under different reaction gases: 9% by volume O_2/Ar, 400 ppmv NO_2 + 9% O_2/Ar.

After the weighing of samples (2mg of soot + 80 mg of SiC), TPO experiments were performed in a U-shaped quartz reactor (internal diameter 8 mm), forming a fixed bed with a depth of approximately 2 mm, on a porous frit. Each sample was placed in the reactor and heated by a thermally isolated furnace from room temperature until 800ºC, with a 10ºC/min ramp. The temperature was monitored by a K-type thermocouple located in a thermowell centred in the particle bed. The temperature program was regulated by a *EUROTHERM 2404* heating controller. Total flow rate through the reactor was maintained at 15 l/h by calibrated *Brooks 5850TR* mass flow controllers. Concentrations of CO and CO_2 (ppmv) present in the outlet gas stream were measured by a *Ultramat 6* analyser.

For each experiment, the carbon specific oxidation rate was normalized to the mass of soot initially introduced in the reactor (V_{spec} in mg/(s.g$_{in}$)) and was calculated with CO and CO_2 emissions (X_{CO} and X_{CO_2} in ppmv) through equation (1). The selectivity of CO_2 (S_{CO_2} in %) in soot oxidation was obtained through equation (2).

$$V_{spec} = \frac{(X_{CO} + X_{CO_2}) \times D \times M_C}{10^6 \times 3600 \times V_M \times m_{C,in}} \qquad (1)$$

$$S_{CO_2} = \frac{X_{CO_2}}{X_{CO} + X_{CO_2}} \times 100 \qquad (2)$$

Where, X_{CO}: CO molar fraction (ppmv), X_{CO_2}: CO_2 molar fraction (ppmv), D: Flow rate (L/h), M_C: Carbon molar mass (mg/mol), V_M: Molar volume = 22,4 L/mol, $m_{C,in}$: initial mass of soot introduced (g).

Trough the obtained curves, temperature of maximal soot oxidation rate (Tm) was collected. Additionally, T_{10}, T_{50} and T_{90} were also determined. These values are the temperatures at which 10, 50 and 90% of carbon soot conversion is reached, respectively. All the carbon present in the samples was assumed to be completely converter into CO and CO_2. ΔT was also calculated, which represents the oxidation interval between 10 and 90% of carbon conversion.

2.3.2. Catalytic oxidation

Soot and MnO_x-CeO_2 mixed oxides (1:4 Mn/Ce molar ratio) were mixed with a weight ratio of 1/10 (2,0 mg/20 mg) by "loose" and "tight" contact. The "loose" contact sample was obtained by mixing the solids with a spatula for 2 minutes. The "tight contact" sample was prepared with a pestle in an agate mortar grinding for 2 minutes too. To minimize the impact of hot spots and to prevent reaction runaway, the soot-catalyst mixture was diluted with 80 mg of SiC powder.

A third type of contact was tested to have an intermediate effect on soot oxidation, between "loose" and "tight" contact. Therefore, the sample was prepared with the same soot/catalyst ratio via using a spatula grinding for 2 minutes and loading about 60 bar pressure in a pneumatic press. The TPO conditions are the same as for non-catalytic oxidation in section 2.3.1.

3. Results and Discussion

3.1. Soot particles characterization

3.1.1. Particles size distribution: Agglomerates

Laser diffraction analysis was used in the present work to determine the size distribution of "model" and "real" soot aggregates. Figure 1 shows the size distribution of soot aggregates obtained through the combustion of biodiesel surrogates with 7% of methyl ester-based additives («MB7», «MO7» and «MD7»), as well as the diesel surrogate «Aref».
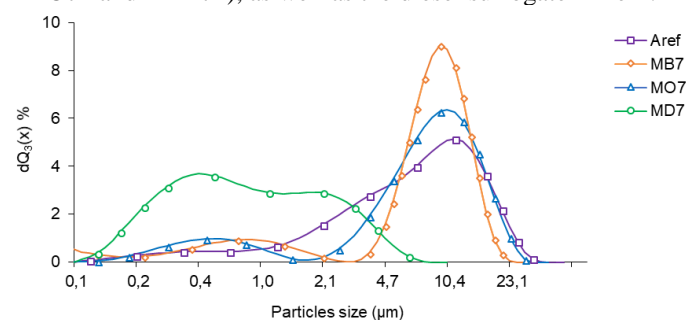

Figure 1. Size distribution of "model" soot aggregates from the diesel surrogate and biodiesel surrogates (7%).

It can be visibly seen that different soot samples show different size distribution profiles. According to the results, when a methyl ester-based additive is added to a diesel surrogate to form a blend with 7% of biodiesel surrogate, the combustion of the fuel produces smaller soot particles. However, this effect is far more relevant when the biodiesel surrogate is composed by molecules with longer carbon chains. In fact, the effect of decreasing particles size is greater when a «MD7» surrogate is used. «Aref» distribution has its principal mode at 11,5 µm, whereas for «MB7» and «MO7» it´s at 10,5 µm. Concerning «MD7» soot, there is a first mode at 0,4 µm and another one at 2,1 µm.

According to the main reaction pathways of CO and CO_2 formation through the pyrolysis and oxidation of methyl esters, proposed by Coniglio *et al.* [41], emissions of CO_2 implies that the oxygen is used to produce this gas instead of inhibiting the atoms of carbon, present in the ester structure, to be available to form soot precursors [42]. Consequently, a better effectiveness in reducing soot precursors and therefore, in reducing soot growth, is attained with the pathways leading to the formation of small amounts of CO_2 coming directly from the decomposition of the methyl ester-based compound. Oxygenated radicals will contribute thereafter to the oxidation of soot precursors and prevent the carbon atoms contained in

the ester structure from becoming available to produce new ones.

Additionally, according to Szybist *et al.* [43,44], the decarboxylation process, which leads to CO_2 formation directly from the oxygenated fuel, just happens after the complete consumption of the aliphatic carbon chain of the methyl ester. Consequently, fuels with long carbon chains (such as «MD» ones) have the production of CO_2 delayed, keeping the oxygenated radicals available in the flame during a longer time and resulting on a more efficient reduction in soot production and growth.

Figure 2 shows the size distribution of different soot samples, namely "models" from the combustion of surrogate with methyldecanoate («MD7» and «MD30») and those obtained on engine bench.
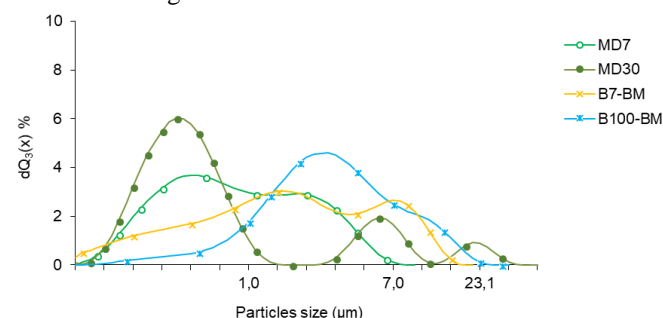

Figure 2. Size distribution of "MD" soot aggregates with 7% and 30% of additives and of "real" soot.

«B7-BM» and «B100-BM» samples present a wide distribution and have two modes. Concerning «B7-BM» soot, two peaks are separately centred at about 1,6 µm and 7 µm. For soot from pure biodiesel, the main peak is about 2,9 µm. In the overall, soot from engine bench seems to have smaller aggregates than "model" soot samples except for those obtained by a surrogate with methyl decanoate («MD7» and «MD30»). Moreover, it is clearly observed that the increase of oxygenated compounds concentration in the biodiesel surrogate leads to the production of smaller particles. Despite the presence of two modes for bigger particles, which is due to the unavoidable agglomeration effect, «MD30» soot agglomerates are globally smaller than «MD7» ones.

These results are consistent with those presented by Lin *et al.* [45], who analysed the impact of different biofuels on the size distribution of soot produced in a HD-vehicle engine. They also concluded that the addition of biodiesel to a diesel fuel promoted a decrease in particles size and an increase in the percentage of small particles. Pyrolysis of fuel with oxygenated compounds leads to the production of O* and OH* radicals, which promote higher oxidation of soot [46,47]. Therefore, the higher the additive content, the higher the oxygen content and consequently, the higher the oxidation process.

In addition to the chemical effect, addition of oxygenated compounds to the diesel surrogate implies the substitution of aromatic compounds (α-MN) by others with less tendency to produce soot precursors. Therefore, the dilution effect leads to the reduction of particles growth through coagulation and surface reactions, due to the low concentration of PAH and acetylene inside the flame [36,48]. Globally, these results illustrate that the combustion of biodiesel surrogate is beneficial to the formation of smaller soot particles aggregates.

3.1.2. Soot composition

The composition of soot particles is a key factor that governs their reactivity. Soot composition was determined by elemental analysis (CHNS/O) and TGA under air and nitrogen for the ash, water and soluble organic fraction (SOF) content. Table 3 shows the composition of soot samples obtained through the combustion of surrogates, diesel and pure biodiesel.

Table 3. Composition of soot.

Sample	%C[1]	%H[1]	%O[1]	%ash[2]	%H2O[3]	%SOF[4]
Aref	87,2	1,0	6,2	0,58	0,59	3,09
MB7	87,4	1,2	4,7	0,39	0,60	3,26
MO7	87,8	0,9	4,4	0,16	0,59	3,01
MD7	89,5	0,9	3,5	0,00	0,45	2,09
MB30	88,3	1,0	4,2	0,52	0,53	3,29
MO30	89,7	1,0	3,6	0,09	0,29	2,39
MD30	91,4	0,8	3,2	0,62	0,37	1,45
B7-BM	89,5	1,2	3,8	1,84	0,28	3,02
B100-BM	83,1	1,3	6,2	7,78	0,42	4,15

[1] Elemental composition CHNS/O
[2] Determined from the mass loss between 30 and 700ºC in TGA under air
[3] Determined from the mass loss between 30 and 110ºC in TGA under nitrogen
[4] Determined from the mass loss between 110 and 400ºC in TGA under nitrogen
The other elements weren´t detected

According to the results, it can be noted that all "model" soot samples have a similar elemental composition. Carbon content is comprised between 87,2 and 91,4 wt%, hydrogen content is around 1 wt% and for oxygen is between 3,2 and 6,2 wt%. A low quantity of water is adsorbed on the soot surface (< 1 wt%) and, in agreement with their production mode, all soot samples have a very low ash content (< 1 wt%). In fact, ash can come from different metallic elements, provided by the additives in the lubrication oil and fuel or by engine wear.

Concerning the carbon content, when the concentration and/or the carbon chain length of oxygenated compounds in the biodiesel surrogate increases, further carbon is introduced. On the contrary, the content of oxygen decreases when the concentration and/or the carbon chain length of such additives increases. For instance, «MD7» soot has 3,5 wt%, while «MD30» one has 3,2 wt%. This means that during their formation, «MD30» particles were subjected to a higher oxidation, leading to a higher consumption of this gas. This phenomenon can be explained by the predominance of soot oxidation over its formation with soot precursors, due to the abundance of oxygenated radicals produced during the pyrolysis of biodiesel surrogate [12-14]. Concerning the carbon chain length, an increase of the number of carbons in the surrogate, lead to a higher residence time of soot particles in the flame and therefore, to a stronger oxidation process, with higher consumption of oxygen.

Finally, the SOF content follows the same tendency as oxygen and seems to be linked to the additive content. In the overall, the content of soluble organic fraction decreases when increasing the concentration of oxygenated compounds and/or their carbon chain length. Both lubricating oil and unburned fuel contribute to the formation of this fraction. It is mainly composed by heavy aromatics compounds, aliphatic chains and oxygenated compounds. Thus, addition of oxygenated additives to the diesel surrogate implies the substitution of aromatic compounds (α-MN) by others with less tendency to produce soot precursors (dilution effect) [36,48]. Concerning the evolution of this fraction in function of the carbon chain length, such occurrence is dependent of each type of molecule and the chemical reactions taking place in the laminar diffusion flame. However, it seems that the longer the carbon chain is, more complete is the combustion in the flame, resulting in a lower amount of SOF content.

Concerning "real" soot, particles from pure biodiesel have a higher oxygen content due to the higher presence of oxygen complexes is this fuel. Consequently, and due to the higher oxidation process, they have a lower carbon content. They also have higher SOF content because of the additives used in biodiesel. Additionally, the increase of biodiesel concentration leads to an increase of the ash content. In fact, «B7-BM» soot has 1,84 wt%, while «B100-BM» has 7,78 wt%. In general, soot from the engine bench has more ash content than the "model" one, due to the presence of additives and corrosion phenomena. On the other hand, an increased biodiesel concentration is generally accompanied by an increase of inorganic compounds content, which promote ash formation.

3.1.3. Raman spectroscopy

In addition to the size and composition, soot nanostructure can also give valuable information about particles formation and oxidation. Therefore, Raman spectroscopy, which is sensitive to molecular structures and to crystalline ones, was used. It generally informs about the abundance of amorphous and graphitized carbon and consequently, about the organization degree in the internal structure of soot.

It has been shown that D1 FWHM and D3 band intensity are the spectroscopic parameters which give most information about the chemical structure and reactivity of different types of soot [49,50]. Table 4 resumes the main results for all samples.

Table 4. FWHM (cm^{-1}) of D1 band, Raman shift (cm^{-1}) of G band and I_{D3}/I_G ratio obtained through Raman spectrums of the studied soot samples.

Soot	D1 FWHM (cm^{-1})	G Raman shift (cm^{-1})	I_{D3}/I_G
Aref	120	1589	0,59
MB7	130	1590	0,62
MO7	126	1590	0,55
MD7	118	1593	0,65
MB30	128	1587	0,59
MO30	121	1591	0,60
MD30	113	1585	0,54
B7-BM	141	1590	0,56
B100-BM	134	1588	0,57

According to the results, the different soot particles have similar structures. The major difference is observed for the D1 FWHM. Concerning "model" soot, it is observed that «MD» particles, and especially «MD30» ones, have the lower FWHM for the D1 band, which demonstrates that their structure may be more ordered [49,50]. About particles collected on engine bench, the Raman results are also very similar. The major difference is also the D1 FWHM, which suggest a higher structural order in «B100-BM» particles than in «B7-BM» ones. Globally, due to the similarity of results between the different samples, Raman spectroscopy is not enough to conclude about significant differences in soot structure and oxidation reactivity. Thus, further studies about the internal structure of soot particles must be carried out.

3.1.4. Length of graphitic layer planes

To assess the reactivity of carbon towards oxidation, analysis of soot structure at the nanometric scale was used. Then, the number and accessibility of edge sites was linked to soot nanostructure. Figure 3 represents the distribution of carbon fringe length of soot particles from different samples, namely from the diesel surrogate «Aref», and from biodiesel

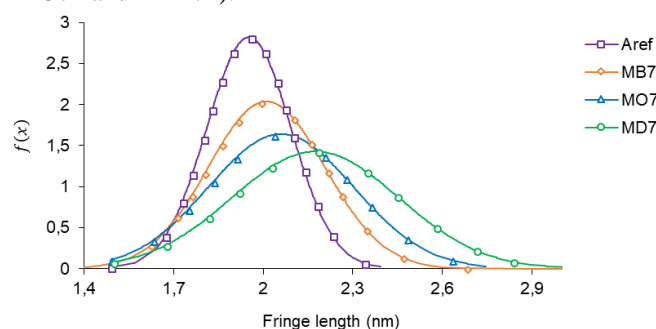surrogates with 7% of methyl ester-based additives («MB7», «MO7» and «MD7»).

Figure 3. Carbon fringe length distribution of soot produced by combustion of the diesel surrogate «Aref» and biodiesel surrogates with 7% of methyl ester-based additives.

«Aref» soot has the narrowest fringe length distribution, with a mean value of 1,95 nm. On the other hand, soot particles obtained from biodiesel surrogates have a larger distribution and at the same time, they have higher mean values of fringe length than the soot of reference. Comparing the different additives, an increase of the fringe length is observed when increasing the length of the carbon chain. The distribution is shifted to higher dimensions and the mean fringe length respects the following order: $L_{«Aref»} < L_{«MB7»} < L_{«MO7»} < L_{«MD7»}$.

It can be suggested that there is a correlation between the fringe length of soot and the length of the aliphatic carbon chain of additives present in the biodiesel surrogate. The longer the chain, the larger the distribution of fringe length and higher the mean value. Thus, it is supposed that an increase in the dimensions of the segments correspond to a lower number of edge sites, higher graphitization and a parallel decrease in oxidation reactivity.

Figure 4 represents the carbon fringe length distribution of soot obtained from the diesel surrogate «Aref», one of the biodiesel surrogates with two different percentages of oxygenate compounds («MD7» and «MD30») and the two "real" soots («B7-BM» and «B100-BM»).
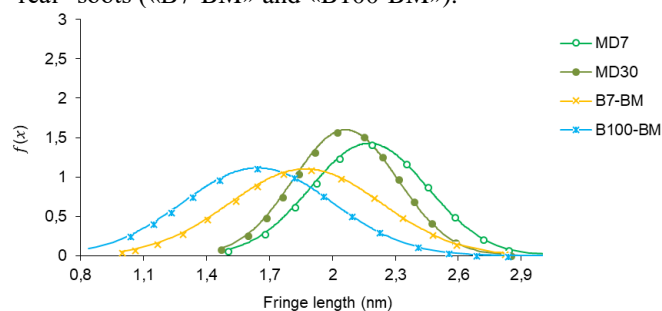

Figure 4. Carbon fringe length distribution of soot produced by combustion of the diesel surrogate «Aref», biodiesel surrogates with 7 and 30% of methyl decanoate and biodiesel (7 and 100%).

«MD7» and «MD30» distributions belong to soot obtained by surrogates that only differ on the oxygenated additive content. As observed, when the percentage of such compounds is increased, the distribution is shifted to smaller fringe length. In fact, with a higher oxygen content, soot is more prone to be oxidized in the flame and consequently, fringes become smaller. Furthermore, the residence time in the flame of «MD30» soot was higher than for «MD7» one, which allowed a better oxidation. Concerning soot particles obtained from the combustion of biodiesel on an engine bench, the same interpretation can be done. «B100-BM» is a pure biodiesel, with a higher oxygen content. Thus, it leads to the formation of soot with shorter fringes than «B7-BM» one [21,36].

3.2. Soot oxidation reactivity

3.2.1. Non-catalytic soot oxidation
3.2.1.1. TPO in 9% by volume O_2/Ar

After the physico-chemical characterisation of soot particles, their oxidation reactivity and therefore, the ease of the DPF regeneration was assessed. A temperature programmed oxidation was carried out with an oxidizer mixture of 9% O_2/Ar, to simulate a non-catalysed DPF active regeneration. «MD7» and «MD30» were used to represent the biodiesel surrogates with 7 and 30% of methyl ester-based additives, respectively. Figure 5 shows the evolution of the carbon specific oxidation rate in function of the temperature. Table 5 displays the main results of the TPO analysis.
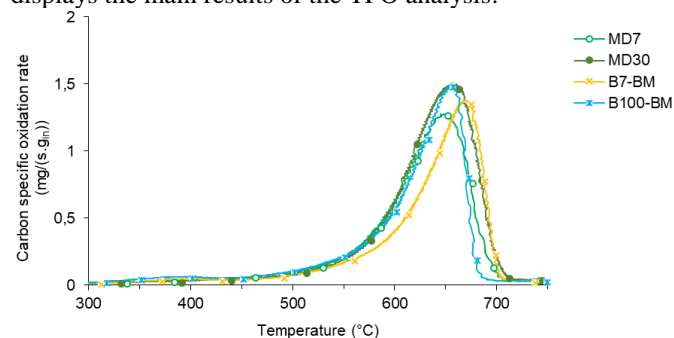

Figure 5. Carbon specific oxidation rate $(mg/(s.g_{in}))$ of "model" and "real" soot (9% O_2/Ar).

Table 5. Temperature programmed oxidation results in 9% b.v. O_2.

	T_m (ºC)	T_{10} (ºC)	T_{50} (ºC)	T_{90} (ºC)	ΔT	S_{CO_2} (%)[1]
MD7	650	498	631	674	176	49
MD30	657	528	640	686	158	47
B7-BM	669	517	647	683	166	55
B100-BM	656	490	631	667	177	69

[1] CO_2 selectivity at T_m

Figure 5 and Table 5 illustrate the oxidative performance of the different samples. It can be observed that all oxidation reactions start at more than 450ºC. In the case of "model" soot, the maximum specific oxidation rate for the «MD7» sample occurs at 650ºC, while 657ºC is attained for the «MD30» one.

In general, reactivity of soot particles decreases when the concentration of oxygenated compounds in the surrogate is increased. These results are coherent with the soot composition obtained through elemental and thermogravimetric analysis. In fact, «MD7» particles contain a higher oxygen and SOF content than the «MD30» ones. The soluble organic fraction provides an easier ignition of soot oxidation, by increasing the internal soot surface with opening and developing of micropores [51,52]. Moreover, previous studies [13,22,53] showed that the incorporation of oxygen in soot particles allowed the formation of oxygenated complexes at the soot surface. Thus, the oxygen content present in soot composition provides a higher oxidation reactivity of these particles. About soot internal structure, Raman spectroscopy proved that «MD30» soot has a more ordered structure, which complicates particles oxidation. In TEM micrographs, it was observed that an increase of oxygenated compounds concentration in the biodiesel surrogate leads to the production of soot particles with a graphitic shell and a less ordered core. It is well known than oxygen reacts easily with the amorphous structure than with the more graphitic one. However, the external structure of «MD30» particles complicates their oxidation.

Concerning the samples produced on engine bench, soot obtained through the combustion of pure biodiesel shows higher oxidation reactivity than soot obtained with

conventional diesel. The maximum carbon specific oxidation rate of «B100-BM» is attained at 656ºC, while 669ºC is obtained for «B7-BM». Furthermore, «B100-BM» samples have a lower ignition temperature (T_{10}) than the «B7-BM» ones. These results are in good agreement with previous works, where was concluded the higher reactivity of biodiesel soot in comparison with diesel soot [13,20,22,54]. This is supported by previous results, such as TEM, Raman and elemental analysis.

Concerning CO and CO_2 emissions, "model" soot was able to produce more carbon monoxide than carbon dioxide, which shows that "model" soot oxidation leads to a less complete oxidation than the "real" one. In terms of "real" soot, a higher biodiesel content, leads to a higher CO_2 formation and a more complete reaction. At the maximum emission temperature (T_m), selectivity of CO_2 for pure biodiesel soot is about 69%, while 55% is found for soot from conventional diesel. The selectivity of CO_2 formation can be explained by the oxygen present in the elemental composition of soot. Indeed, the order of soot oxygen content is the following one: «MD30» < «MD7» < «B7-BM» < «B100-BM», which corresponds to the same order of carbon dioxide selectivity.

3.2.1.2. TPO in 400 ppmv NO_2 + 9% O_2/Ar

In soot-NO_2-O_2 reaction systems, a cooperative reaction of the two gases with soot carbon allows a better soot oxidation. In order to observe this cooperative action, a temperature programmed oxidation was carried out with an oxidizer mixture of 400 ppmv NO_2 + 9% O_2/Ar. Figure 6 shows the evolution of the carbon specific oxidation rate in function of the temperature. Soot conversion profiles are resumed in Table 6.
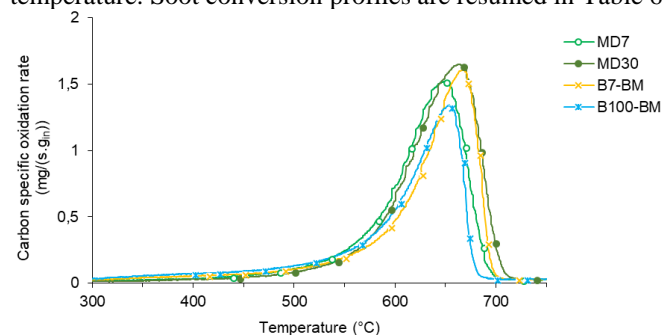

Figure 6. Carbon specific oxidation rate (mg/(s.g$_{in}$)) of "model" and "real" soot (400 ppmv NO_2 + 9% O_2/Ar).

Table 6. Temperature programmed oxidation results in 400 ppmv NO_2 + 9% b.v. O_2.

	T_m (°C)	T_{10} (°C)	T_{50} (°C)	T_{90} (°C)	ΔT	S_{CO_2} (%)[1]
MD7	648	528	631	671	143	35
MD30	664	551	643	683	132	35
B7-BM	667	509	644	681	172	51
B100-BM	654	457	626	666	209	64

[1] CO_2 selectivity at T_m

Through the analysis of Figure 6 and Table 6, it can be seen that the TPO profiles and CO_2 selectivity are similar to those under O_2. In fact, no significant decrease of the maximal soot oxidation temperature (T_m) was promoted by the presence of NO_2 in the reaction gas. However, the temperature to obtain 10% of carbon conversion showed considerable modifications. For "model" soot «MD7» and «MD30», a visible increase of T_{10} can be observed. On the contrary, "real" soot samples present lower values. Such results reveal that NO_2 more easily promotes the oxidation of soot generated on engine bench. This behaviour can be attributed to the oxidation of the soluble organic fraction (SOF) by this gas. Mainly due to the presence of lube oils and unburned fuel, soot produced through engine

combustion processes («B7-BM» and «B100-BM») contain a higher SOF content, formed on the soot particle surface, than the soot produced with the Santoro burner. These findings are in good agreement with previous investigations. Several studies demonstrated the stronger oxidation power of NO_2 in comparison with O_2 at low temperatures (<450ºC). However, high temperatures lead to the decomposition of NO_2 into NO and thereby make NO_2 loose its promoting role [55,56]. This phenomenon can explain the absence of decrease of T_m with addition of NO_2 in the reaction gas.

3.2.1. Catalytic soot oxidation

The use of oxidative catalysts to lower the combustion temperature for soot abatement is believed to be a feasible and promising method in reducing soot emission. Consequently, a temperature programmed oxidation was carried out with an oxidizer mixture of 9% O_2/Ar, in "loose contact" conditions. Figure 7 shows the evolution of the carbon specific oxidation rate in function of the temperature. Table 7 exhibits the main results of the TPO analysis.
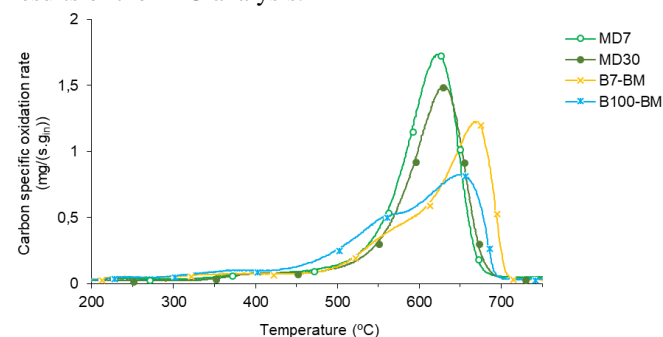

Figure 7. Carbon specific oxidation rate (mg/(s.g$_{in}$)) of "model" and "real" soot in presence of MnO_x-CeO_2 mixed oxides (9% O_2/Ar), in "loose" contact.

Table 7. Temperature programmed oxidation results in 9% O_2/Ar in presence of mixed oxides, in "loose" contact.

	T_m (°C)	T_{10} (°C)	T_{50} (°C)	T_{90} (°C)	ΔT	S_{CO_2} (%)[1]
MD7	621	405	606	651	246	99
MD30	631	457	614	658	201	99
B7-BM	672	407	629	683	276	99
B100-BM	652	383	592	667	284	99

[1] CO_2 selectivity at T_m

The introduction of mixed oxides catalysts in the reaction bed allowed to a significant decrease of T_{10}. However, the temperature of maximal oxidation rate didn´t decrease as much as expected, even if these oxides are considered good oxygen carriers. Soot oxidation under oxygen strongly depends of soot/catalyst contact. "Loose contact" conditions are characterized by a low number of contact points between soot particles and MnO_x-CeO_2 mixed oxides. Consequently, it is expectable to have a reduced catalytic performance [57,58].

Regarding CO_x emissions, the introduction of a catalyst into the reaction bed promoted CO_2 formation from carbon oxidation instead of CO, leading to a complete reaction. Indeed, for all soot samples, a CO_2 selectivity of 99% was obtained.

Due to the low catalytic activity in soot oxidation under "loose" contact between MnO_x-CeO_2 mixed oxides and soot samples, the effect of soot-catalyst contact was evaluated through the comparison between three different contact degrees. Figure 8 shows the evolution of the carbon specific oxidation rate in function of the temperature, for «MD30» sample.
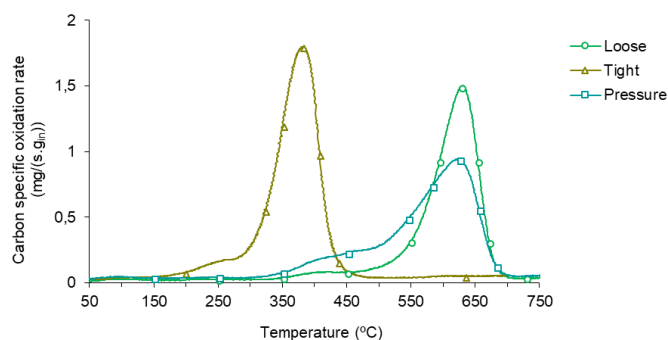
Figure 8. Carbon specific oxidation rate (mg/(s.g$_{in}$) of «MD30» soot in presence of MnO$_x$-CeO$_2$ mixed oxides (9% O$_2$/Ar).

According to the results, it can be observed that soot oxidation temperatures are shifted to much lower values and the TPO curves become narrower in "tight" contact conditions. Concerning experiments under "pressure" contact, a wider temperature window is present, with a lower reaction rate. As expected, it represents an intermediate contact condition. The two peaks shape is probably due to the heterogeneity of the soot-catalyst mixture.

An order of reactivity can be established in function of the contact conditions between soot samples and MnO$_x$-CeO$_2$ mixed oxides: "Loose" contact < "Pressure" contact < "Tight" contact. The tightness of the contact between the two solids and therefore, the number of contact points, is a critical factor for the enhancement of catalytic soot oxidation. From "loose" contact to "tight" contact conditions, the temperature of maximal soot oxidation rate is decreased of, at least, 250ºC. The interface between the two solids is limited by the contact points between larger soot particles and larger clusters of catalyst particles [59,60]. Since the action of the catalyst on carbon oxidation is mainly linked to the proximity of the carbon active sites to those of the catalyst and to the number of active sites accessible for the reaction gas, "loose" contact conditions provide a higher interfacial area between the two solids and a reduced catalytic activity.

4. Conclusion

The laser diffraction analysis allowed to measure the particles mean granulometry. It was deduced that the presence of oxygenated compounds with a higher concentration and/or carbon chain length leads to the production of smaller particles. Indeed, «MD30» particles presented the smaller mean size. Furthermore, elemental and Raman analyses proved that «MD30» soot had the smallest oxygen and SOF content and a more ordered structure. TEM measurements showed that the mean carbon fringe length increases with the ester chain length but decreases with the Biodiesel content. In sum, all these tests showed that the structure and composition of soots depend on the fuel nature.

Concerning oxidation experiments (TPO) under O$_2$ and O$_2$+NO$_2$, it was deduced that the reactivity of soot particles decreases when the concentration of oxygenated compounds in the surrogate increases. Furthermore, in terms of "real" soot, biodiesel particles were more reactive than the diesel ones. No significant decrease of the maximal soot oxidation temperature was promoted by the presence of NO$_2$. However, the temperature to obtain 10% of carbon conversion showed considerable modifications. This temperature decreased in the case of "real" soot, probably due to the oxidation of the soluble organic fraction (SOF) by this gas.

Finally, the impact of the soot-catalyst interaction was assessed. The presence of MnO$_x$-CeO$_2$ mixed oxides facilitated the reaction at lower temperatures and led to a complete soot oxidation, with a CO$_2$ selectivity of almost 100%. Three contact conditions were tested and compared. As expected, due to the tightness of the contact between soot and the catalyst, oxidation under "tight" contact conditions allowed to a decrease of the temperature of maximal soot oxidation rate about, at least, 250ºC.

To conclude, it was proved that the properties and characteristics of soot can give some information and be correlated with the oxidation reactivity. Furthermore, despite some differences, it can be considered that with the experimental installation used to produce "model" soot, it is possible to generate particles with properties close to those of "real" ones. Thus, "model" soot can be considered as representative of soot produced under real driving conditions and be used for further studies. However, numerous improvements should be made to better understand to soot formation and oxidation process.

5. Future Work Proposals

Based on the results and conclusions achieved through this work, there are some aspects which future study may be of interest.

- X-ray diffraction (XRD) analysis, to obtain a quantitative analysis of the graphitization degree and therefore, to better correlate soot structure with oxidation reactivity.

-TPO experiments under pure NO$_2$, in presence or not of catalyst.

-TPO experiments under NO+O$_2$, in presence of catalyst, to understand the interaction between NO and the catalyst surface.

-DRIFT spectroscopy analysis, to identify the intermediates formed during soot oxidation. Thus, role of NO$_2$, NO and O$_2$ in soot oxidation can be identified and the mechanism can be confirmed.

-BET experiments, to do a surface area analysis and to do a correlation between the oxidation reactivity and surface area.

-Improvement of the experimental device used to produce and collect the tested "model" soot, to work under moderated pressure (1-10 bar). It would allow to get closer to the real process of soot production and therefore, to evaluate the impact of pressure on the formation, physico-chemical properties and reactivity of particles. Furthermore, collection of soot samples at different heights of the flame could also be interesting.

-Impregnation of alkali metals (Na, K, …) on "model" soot, in order to study the impact of soot properties and oxidation reactivity. In real conditions, such inorganic compounds come from NaOH and KOH catalysts, used during the production of biodiesel. Furthermore, soots can also contain other elements, coming from lubricant oils in diesel engines, such as Ca, Zn, Fe and Mg. It should be interesting to evaluate the impact of each compound on soot reactivity.

-X-ray photoelectron spectroscopy (XPS), to identify and quantify trace elements, carbon oxidation state (oxygen functional groups, to identify the degree of oxidation)

-Impregnation of platinum or palladium in the mixed oxides structure, to observe its promotion on NO oxidation activity. In fact, the main oxidation function of such metals is indirect by converting NO to NO$_2$.

6. References

[1] *Explaining road transport emission*, European Environment Agency, Copenhaga, **2016**.

[2] P. T. O. Shaughnessy, "Occupational health risk to nanoparticulate exposure", *Environ. Sci. : Processes Impacts*, **2013**,15, pp. 49-62.

[3] Heavy-Duty Emissions, February 2018, https://www.transportpolicy.net/topic/emissions-standards/

[4] C. Escobar, E. S. Lora, O. J. Venturini, E. E.Yáñez, E. F. Castillo and O. Almazan, "Biofuels : Environment , technology and food security," *Renewable and Sustainable Energy Reviews*, **2009**, 13(6-7), pp. 1275-1287.

[5] C.D. Rakopoulos, D.C. Rakopoulos, D.T. Hountalas, E.G. Giakoumis, E.C. Andritsakis, "Performance and emissions of bus engine using blends of diesel fuel with bio-diesel of sunflower or cottonseed oils derived from Greek feedstock", *Fuel*, **2008**, 87(2), pp.147-157.

[6] A. L. Boehman, J. Song, and M. Alam, "Impact of Biodiesel Blending on Diesel Soot and the Regeneration of Particulate Filters", *Energy & Fuels*, **2005**, 19, pp. 1857-1864.

[7] W. G. Wang, D. W. Lyons, N. N. Clark, and M. Gautam, "Emissions from Nine Heavy Trucks Fueled by Diesel and Biodiesel Blend without Engine Modification", *Environmental Science & Technology*, **2000**, 34, pp. 933-939.

[8] J. Rodríguez-Fernandez, M. Lapuerta, J. Sanchez-Valdepenas, "Regeneration of diesel particulate filters: Effect of renewable fuels", *Renewable Energy*, **2017**, 104, pp. 30-39.

[9] D. Fino, V. Specchia, "Open issues in oxidative catalysis for diesel particulate abatement", *Powder Technology*, **2008**, 180, pp. 64-73.

[10] A-M. Stamatellou, A. Stamatelos, "Overview of Diesel particulate filter systems sizing approaches", *Applied Thermal Engineering*, **2017**, 121, pp. 537-546.

[11] M. Lapuerta, J. Rodríguez-Fernández, F. Oliva, "Effect of soot accumulation in a diesel particle filter on the combustion process and gaseous emissions", *Energy*, **2012**, 47(1), pp.543-552.

[12] Z. Du, "Kinetic Modeling of Carbon Oxidation", PhD Thesis, Massachusetts Institute of Technology, **1990**.

[13] H. J. Seong, A. L. Boehman, "Studies of soot oxidative reactivity using a diffusion flame burner", *Combust and Flame*, **2012**, 159(5), pp.1864-1875.

[14] K. C. Lin, J. Y. W. Lai and A. Violi, "The role of the methyl ester moiety in biodiesel combustion: A kinetic modelling comparison of methyl butanoate and n-butane", *Fuel*, **2012**, 92(1), pp.16-26.

[15] P. F. Flynn *et al.*, "Diesel Combustion: An Integrated View Combining Laser Diagnostics, Chemical Kinetics, And Empirical Validation," *SAE Technical Paper*, **1999**.

[16] K. Schmidt, J. Van Gerpen, "The Effect of Biodiesel Fuel Composition on Dieel Combustion and Emissions", *SAE Technical Paper*, **1996**.

[17] C. Mueller, W. Pitz, L. Pickett, G. Martin et al., " Effects of Oxygenates on Soot Processes in DI Diesel Engines: Experiments and Numerical Simulations", *SAE Technical Paper*, **2003**.

[18] R.L. Vander Wal, A. J. Tomasek, "Soot oxidation: dependence upon initial nanostructure", *Combustion and Flame*, **2003**, 134(1-2), pp. 1-9.

[19] J.-O. Müller, D. S. Su, R. E. Jentoft, U. Wild, and R. Schlögl, "Diesel Engine Exhaust Emission: Oxidative Behavior and Microstructure of Black Smoke Soot Particulate", *Environmental Science and Technol*ogy, **2006**, 40(4), pp.1231-1236.

[20] J. Song, M. Alam, A. L. Boehman, U. Kim, "Examination of the oxidation behavior of biodiesel soot", *Combustion and Flame*, **2006**, 146(4), pp.589-604.

[21] R.L. Vander Wal, A. J. Tomasek, "Soot nanostructure: dependence upon synthesis conditions", *Combustion and Flame*, **2004**, 136(1-2), pp.129-140.

[22] J. Song, M. Alam, A. Boehman, "Impact of alternative fuels on soot properties and DPF regeneration", *Combustion Science and Technology*, **2007**, 179(9), pp. 1991-2037.

[23] K. Chen, K.S. Martirosyan, D. Luss, "Transient temperature rise during regeneration of diesel particulate filters", *Chemical Engineering J*ournal, **2011**, 176-177, pp.144-150.

[24] V. Palma, P. Ciambelli, E. Meloni, A. Sin, "Catalytic DPF microwave assisted active regeneration", *Fuel*, **2015**, 140, pp. 50-61.

[25] H. Muroyama, S. Hano, T. Matsui, K. Eguchi, "Catalytic soot combustion over CeO$_2$-based oxides", *Catalysis Today*, **2010**, 153(3-4), pp. 133-135.

[26] F. Lin, X.D. Wu, S. Liu, D. Weng, Y.Y. Huang, "Preparation of MnO$_x$-CeO$_x$-Al$_2$O$_3$ mixed oxides for NOx-assisted soot oxidation: Activity, structure and thermal stability", *Chemical Engineering J*ournal, **2013**, 226, pp.105-112.

[27] A. Bueno-López, K. Krishna, M. Makkee and J.A. Moulijn, "Active oxygen from CeO$_2$ and its role in catalysed soot oxidation", *Catalysis Lett*ers, **2005**, 99(3-4), pp. 203-205.

[28] W.J. Shan, N. Ma, J.L. Yang, X.D. Wu, C. Liu, L.L. Wei, "Catalytic oxidation of soot particulates over MnO$_x$-CeO$_2$ oxides prepared by complexation-combustion method", *J*ournal of Natural Gas Chemistry, **2010**, 19(1), pp. 86-90.

[29] X.D. Wu, F. Lin, H.B. Xu, D. Weng, "Effects of absorbed and gaseous NOx species on catalytic oxidation of diesel soot with MnO$_x$-CeO$_2$ mixed oxides", *Applied Catalysis B: Environmental*, **2010**, 96(1-2), pp. 101-109.

[30] L. Xueting, L. Shujun, H. Hui, W. Zeng, W. Junliang, C. Limin, Y. Daiqi, F. Mingli, "Evolution of oxygen vacancies in MnO$_x$-CeO$_2$ mixed oxides for soot oxidation", *Applied Catalysis B: Environmental*, **2018**, 223, pp. 91-102.

[31] X. Wu, F. Lin, H. Xu, D. Weng, "Effects of adsorbed and gaseous NOx species on catalytic oxidation of diesel soot with MnO$_x$-CeO$_2$ mixed oxides", *Applied Catalysis B: Environmental*, **2010**, 96(1-2), pp. 101-109.

[32] M. M. Fiuk, A. Adamski, "Activity of MnO$_x$-CeO$_2$ catalysts in combustion of low concentrated methane", *Catalysis Today*, **2015**, 257(1), pp. 131-135.

[33] K. Tikhomirov, O. Kröcher, M. Elsener, AA. Wokaun, "MnO$_x$-CeO$_2$ mixed oxides for the low-temperature oxidation of diesel soot", *Applied Catalysis B: Environmental*, **2006**, 64(1-2), pp. 72-78.

[34] A. Setiabudi, J.L. Chen, G. Mul, M. Makkee, J.A. Moulijin, "CeO$_2$ catalysed soot oxidation. The role of active oxygen to accelerate the oxidation conversion", *Applied Catalysis B: Environmental*, **2004**, 51(1), pp. 9-19.

[35] R. J. Santoro, H. G. Semerjian, and R. A. Dobbins, "Soot Particle Formation in Diffusion Flames," *Combust. Flame*, **1987**, pp. 513-523.

[36] R. Lemaire, D. Lapalme and P. Seers, "Analysis of the sooting propensity of C-4 and C-5 oxygenates: Comparison of sooting indexes issued from laser-based experiments and group additivity approaches", *Combustion and Flame*, **2015**, 162, pp.3140-3155.

[37] H. P. Ramirez, K. Hadj-Ali, P. Diévart, G. Moréac and

P. Dagaut, "Kinetics of Oxidation of Commercial and Surrogate Diesel Fuels in a Jet-Stirred Reactor: Experimental and Modeling Studies", *Energy Fuels*, **2010**, 24(3), pp. 1668-1676.

[38] J. Abboud, J. Schobing, G. Legros, J. Bonnety, V. Tschamber, A. Brillard, G. Leyssens, V. Lauga, E. E. Iojoiu, P. Da Costa, "Impacts of oxygenated compounds concentration on sooting propensities and soot oxidative reactivity: Application to Diesel and Biodiesel surrogates", *Fuel*, **2017**, 193, pp. 241-253.

[39] C. S. McEnally, L. D. Pfefferle, "Sooting tendencies of oxygenated hydrocarbons in laboratory-scale flames", *Environmental Science and Technology*, **2011**, 45(6), pp.2498-2503.

[40] M. Kashif, P. Guibert, J. Bonnety, G. Legros, "Sooting tendencies of primary reference fuels in atmospheric laminar diffusion flames burning into vitiated air", *Combustion and Flame*, **2014**, 161(6), pp. 1575-1586.

[41] L. Coniglio, H. Bennadji, P. A. Glaude, O. Herbinet, and F. Billaud, "Combustion chemical kinetics of biodiesel and related compounds (methyl and ethyl esters): Experiments and modeling e Advances and future refinements," *Prog. Energy Combust. Sci.*, **2013**, 39(4), pp. 340–382.

[42] H.L. Zhang, S. Yuan, J. L. Wang, M. C. Gong and Y.Q. Chen, "Effects of contact model and NOx on soot oxidation activity over Pt/MnO_x-CeO_2 and the reaction mechanisms", *Chemical Engineering Journal*, **2017**, 327, pp. 1066-1076.

[43] C. K. Westbrook, W. J. Pitz and H. J. Curran, "Chemical Kinetic Modeling Study of the Effects of Oxygenated Hydrocarbons on Soot Emissions from Diesel Engines", The *Journal of Physical Chemistry*, **2006**, 110(21), pp. 6912-6922.

[44] J. P. Szybist, A. L. Boehman, D. C. Haworth and H. Koga, "Premixed ignition behaviour of alternative diesel fuel-relevant compounds in a motored engine experiment", *Combust Flame*, vol.149, no.1-2, pp.112-128, 2007.

[45] J. P. Szybist, J. Song, M. Alam and A. L. Boehman, "Biodiesel combustion, emissions and emission control", *Fuel Processing Technology*, **2007**, 88(7), pp.679-691.

[46] E. J. Barrientos, M. M. Maricq, J. E. Anderson, "Impact of ester structures on the soot characteristics and soot oxidative reactivity of biodiesel", *SAE Techical Paper*, **2015**.

[47] Y-C. Lin, C-F. Lee and T. Fang, "Characterization of particle size distribution from diesel engines fueled with palm-biodiesel blends and paraffinic fuel blends", *Atmospheric Environment*, **2008**, 42, pp.1133-1143.

[48] P. Pepiot-Desjardins, H. Pitsch, R. Malhotra, S.R. Kirby and A.L. Boehman, "Structural group analysis for soot reduction tendency of oxygenated fuels", *Combustion and Flame*, **2008**, 154, pp.191-205.

[49] M. Knauer, M. E. Schuster, D. Su, R. Schlogl, R. Niessner and N. P. Ivleva, "Soot Structure and Reactivity Analysis by Raman Microspectroscopy, Temperature-Programmed Oxidation, and High-Resolution Transmission Electron Microscopy", *The Journal of Physical Chemistry A*, **2009**, 113(50), pp. 13871-13880.

[50] J. Schmid, B. Grob, R. Niessner and N. P. Ivleva, "Multiwavelength Raman Microspectroscopy for Rapid Prediction of Soot Oxidation Reactivity", *Analytical Chemistry*, **2011**, 83(4), pp. 1173-1179.

[51] Z. Ma, L. Li, Y. Chao, N. Kang, B. Xu and J. Wu, "Effects of Diesel Oxidation Catalyst on Nanostructure and Reactivity of Diesel Soot", *Energy & Fuels*, **2014**, 28(7), pp.4376-4382.

[52] A. W. Kandas, I. G. Senel, Y. Levendis and A. F. Sarofim, "Soot surface area evolution during air oxidation as evaluated by small angle X-ray scattering and CO_2 adsorption", *Carbon*, 2005, 43(2), pp. 241-251.

[53] J. Song, M. Alam and A. L. Boehman, "Characterization of Diesel and Biodiesel soot", *Prepr. Pap.-Am. Chem. Soc. Div. Fuel Chem.*, **2004**, 49(2), pp.767-769.

[54] M. N. Ess, H. Bladt, W. Mühlbauer, S. I. Seher, C. Zöllner, S. Lorenz et al., "Reactivity and structure of soot generated at varying biofuel content end engine operating parameters", *Combustion and Flame*, **2016**, 163, pp. 157-159.

[55] A. Setiabudi, BAAL. van Setten, M. Makkee, J. A. Moulijn, "The influence of NO_x on soot oxidation rate: molten salt versus platinum", *Applied Catalysis B: Environmental*, **2002**, 35(3), pp.159-166.

[56] B.R. Stanmore, J.F. Brilhac, P. Gilot, "The oxidation of soot: a review of experiments, mechanisms and models", *Carbon*, **2001**, 39(15), pp. 2247-2268.

[57] M. Issa, C. Petit, A. Brillard and J.F. Brilhac, "Oxidation of carbon by CeO_2: Effect of the contact between carbon and catalytic particles", *Fuel*, **2008**, 87(6), pp.740-750.

[58] N. Zouaoui, M. Issa, D. Kehrli and M. Jeguirim, "CeO_2 catalytic activity for soot oxidation under NO/O2 in loose and tight contact", *Catalysis Today*, **2012**, 189(1), pp.65-69.

[59] J. Christensen, J-D. Grunwaldt and A. D. Jensen, "Importance of the oxygen bond strength for catalytic activity in soot oxidation", *Applied Catalysis B: Environmental*, **2016**, 188, pp.235-244.

[60] D. Gardini, J. M. Christensen, C. D. Damsgaard, A. D. Jensen and J. B. Wagner, "Visualizing the mobility of silver during catalytic soot oxidation", *Applied Catalysis B: Environmental*, **2016**, 183, pp.28-36.